scientific reports

Check for updates

OPEN

The relationship between acid-sensing ion channel, *ASIC2*, and oncogenic β-catenin signaling in ovarian cancer

Tanvi Joshi[1], Sagar Chokshi[1], Annelise Wilhite[2], Mary Howard Singleton[1], Elizabeth Catranis[1], Jennifer Scalici[3] & Kevin J. Lee[1]✉

Inflammation associated with incessant ovulation plays a key role in epithelial ovarian cancer (EOC) pathogenesis. Ion channels, such as acid-sensing ion channel-2 or *ASIC2* are known to be upregulated in inflammatory conditions and may play a role in cancer cell invasion and metastasis. Previously we reported the role of phosphodiesterase 10A (PDE10) modulation of β-catenin in ovarian cancer, and are currently investigating its contribution to ovarian pathogenesis. Differential ASIC2 expression was noted with PDE10 modulation in both pre-malignant and ovarian cancer tissues. Hence, we presently report the potential role of *ASIC2* in EOC development and progression as well as involvement with PDE10. ASIC2 protein is expressed across all EOC cell lines, primarily within the nucleus. Knockout of PDE10 decreased ASIC2. Conversely, ASIC2 inhibition decreased ASIC2 as well as PDE10 protein levels. ASIC2 inhibition via Diminazene also produced marked ovarian cancer death. While changes in extracellular pH did not impact ASIC2 expression, intracellular pH and calcium levels increased with ASIC inhibition. Calcium increases induced a decrease in oncogenic β-catenin. There may be a direct relationship between PDE10 and ASIC2 protein expression in EOC through convergence on a β-catenin mediated signaling pathway. This could potentially implicate ion channels, specifically ASIC2, as a link between the acidic tumor microenvironment and cancer cell signaling. It is also possible that ASIC2 plays a crucial role in acidosis-mediated tumorigenesis in ovarian cancer.

Keywords ASIC2, PDE10, Ovarian cancer, Calcium channel, B-catenin

Epithelial ovarian cancer (EOC) presents at advanced stages in roughly 80% of patients[1,2]. Efforts at early detection to reduce mortality have been largely unsuccessful as the pathogenesis of EOC remains unclear[2–4]. It is now increasingly accepted that high-grade serous cancers may originate in the fallopian tube and may exfoliate to the adjacent ovary and surrounding structures[5]. The inflammatory microenvironment shared by the ovary and the distal fallopian tube (FT), particularly in the context of ovulation, can contribute to the development of EOC[5,6].

Further evidence supporting this theory are the numerous studies that suggest that nonsteroidal anti-inflammatory drugs (NSAIDs) have a preventive effect on the development of ovarian cancer[7–9]. Evolving literature suggests that the anticancer properties of NSAIDs are mediated in a cyclooxygenase (COX)-independent manner via the blockade of phosphodiesterases (PDEs)[10]. We previously reported on the expression of PDE10, an enzyme unique to the ovary[11]. PDE10 was shown to modulate a variety of oncogenic pathways to increase tumorigenesis of ovarian cancer in vivo and in vitro[11]. To understand the role of PDE10 in the inflammatory environment of ovarian cancer, it is essential to understand the role of ion channels which may be an integral component of the acidic tumor microenvironment[12].

Acid-sensing ion channels (ASIC) are a group of transmembrane channels that allow for the influx of cations during inflammatory conditions[13]. There are at least eight ASIC subunit proteins, encoded by five genes that have been identified[14,15]. These channels have been shown to be sensitive to small or moderate pH reductions in the brain during both physiologic and pathologic conditions[16]. Activation of ASICs can induce neuronal injury during prolonged periods of acidosis such as brain injury or stroke[17].

[1]USA Health Mitchell Cancer Institute, University of South Alabama, 1660 Springhill Ave, Mobile, AL 36604, USA. [2]Carilion Clinic, Virginia Tech School of Medicine, Roanoke, VA, USA. [3]Emory University School of Medicine, Atlanta, GA, USA. ✉email: kjlee@health.southalabama.edu

ASICs have also recently been identified as important mediators in other inflammatory states such as cancer progression and metastasis[18]. ASICs have been shown to be upregulated in breast, pancreatic, gastric and hepatocellular carcinomas[18–21]. In colorectal cancer, ASIC2 was shown to induce proliferation and metastasis in vitro as well as in vivo through calcium increase and activation of nuclear factor of activated t-cells (NFAT) signaling[21]. In breast cancer, ASIC1 mediated primary tumor growth and was highly expressed in malignant tissues relative to control[20]. Furthermore, inhibition or genomic knock-out of ASIC-1 expression induced liver cancer cell apoptosis[21]. Additionally, ASIC-1 was shown to play an integral part in glioblastoma cell function in conjunction with epithelial sodium channels[22].

Therefore, the goal of the present study was to investigate the role of ASIC2 in ovarian cancer, where inflammation and acidosis may be important mediators. We report ASIC2 expression in human ovarian cancer cell lines and its potential role in mediating intracellular calcium and cancer cell viability. We also investigate a potential relationship between PDE10 and ASIC2 in ovarian cancer and the role it plays in oncogenic β-catenin signaling.

Methods

Cell lines

Immortalized human epithelial ovarian cancer cell lines, ES2, OVCAR8 and SKOV3 were obtained from ATCC and were grown to sub-confluence in a 37 °C humidified incubator with 5% CO2. ES2 and SKOV3 were maintained in McCoy's media supplemented with 10% Fetal Bovine Serum (FBS) and 1% Penicillin-Streptomycin (P-S). OVCAR8 was maintained in RPMI supplemented with 10% FBS and 1% P-S. All cell lines were determined to be free of mycoplasma and expanded into numerous aliquots upon receiving and stored in liquid nitrogen.

TCGA analysis

ASIC2 mRNA expression and clinical survival data for ovarian cancer patients was downloaded from The Cancer Genome Atlas (TCGA) using cBioPortal. The mRNA comparison tool in the cBioportal was used to compare TCGA ovarian tumors in TCGA, firehouse legacy dataset with a total of 617 samples. Initially, PDE10 mRNA expression was divided into quartiles and comparisons were made between the PDE10 High expression group and the PDE10 Low expression group. Within those subsets ASIC2 expression was analyzed and comparisons were made between ASIC2 expression in the PDE10 Low group and ASIC2 expression in the PDE10 High group.

Immunohistochemistry

Prior to plating cells in 8-well chambered coverglass, EmbryoMax 0.1% gelatin solution (Millipore) was added and allowed to incubate for a minimum of 10 min at room temperature (RT). Gelatin solution was removed and ovarian cancer cells (ES2, OVCAR8, and SKOV3) were plated at 15,000 cells per well and allowed to adhere overnight. Once cells reached 60–70% confluency, treatments were added as indicated and cells were then fixed in 4% formaldehyde for 10 min at RT. Cells were then washed in Phosphate Buffered Saline (PBS) X3 and permeabilized with Permeabilization Buffer (Biotium) for 10 min at RT. Cells were washed in PBS X3 and blocked with 2% bovine serum albumin (BSA) in PBS for 30 min at RT followed by incubation with primary antibody overnight at 4 °C. Primary antibodies were used to detect ASIC2 (ThermoFisher #PA5-26222), non-phospho-β-catenin S45 (CellSignaling #19807, RRID: AB_2650576), non-phospho-β-catenin S33/37/T41 (CellSignaling #8814, RRID: AB_11127203), C-MYC (CellSignaling #5605, RRID: AB_1903938) IgG (abcam #ab171870, RRID: AB_2687657). The following day cells were washed in PBS X3 and incubated with AlexaFluor-488 anti-rabbit (a11008 LifeTech) at 1:500 for 1 h at RT. Hoechst was then added as a nuclear stain at a dilution of 1:3,000 for 15 min. Cells were then washed in PBS X3 and imaged.

Western blot analysis

Cell lysates (30 µg of protein per lane) were separated by polyacrylamide gel (10–15%) electrophoresis and transferred to nitrocellulose membranes. Membranes were then blocked with 5% milk in Tris-Buffered Saline (TBS) containing 1% Tween (TBS-T). Membranes were incubated overnight at 4 °C with the relevant primary antibody (ASIC2 pa5-26222 Life Tech 1:500; PDE10 ab227829 Abcam 1:500, RRID: AB_2927552; Actin a2228 Sigma 1:10,000, RRID: AB_476697; GAPDH 2118 Cell Signaling 1:5,000, RRID: AB_561053). Membranes were washed with TBS-T and an HRP-secondary antibody was added for 1 h at room temperature on an orbital shaker. The membranes were then washed again with TBS-T three times prior to imaging. HRP-secondary antibodies were detected by incubating with WesternBright Sirius chemiluminescence.

Cell viability luminescence assay

Cells were plated in 96-well black-wall, clear-bottom tissue culture plates at a concentration of 1,000 cells/well and allowed to adhere overnight. Cells were then treated with ASIC inhibitors (Diminazine, Selleck Chemicals; Amiloride, Selleck Chemicals) for 72 h at 37 °C (5% CO2). Cell viability was measured with CellTiter-Glo Assay (Promega) as per manufacturer's protocol. Luminescence reading was performed with the use of a Synergy H4 Hybrid Reader (Biotek). Cells were treated with vehicle control in parallel with inhibitors and data were normalized to vehicle control for all doses treated presented as percent (%) survival. Dose-response curves and IC50 values were calculated on GraphPad Prism 8.

pH studies

Global extracellular pH was changed with the use of hydrochloric acid (HCl) over various time points: 2 h, 4 h, 8 h, 12 h and 24 h. Extracellular pH was measured with the use of a standard pH meter. The pH of cell media was

increased to 6.0 and 6.5. ASIC2 expression was subsequently measured via western blot. Intracellular pH was determined with the use of pH-sensitive pHrodo red dye kit (Life Technologies). Cellular pH was measured per the manufacturer's protocol in cell lines at baseline and after treatment with 10 μM Diminazene over 30 min and 2 h. Live cell imaging was utilized on a Nikon A1r confocal microscope.

Calcium studies

Intracellular calcium levels were measured with the use of a Fluo Calcium Indicator kit (ThermoFisher) per manufacturer's protocol in cell lines at baseline and after treatment with 10 μM Diminazene over 30 min and 2 h. Briefly, 15,000 cells were plated in chambered cover-slides and allowed to grow overnight at 37 °C (5% CO2) before initialization of experiments. Live cell imaging was utilized on a Nikon A1r confocal microscope.

Image acquisition and analysis

All images for confocal IHC and pH and calcium studies were acquired using a Nikon A1r scanning confocal microscope with a 20x objective. Gain settings for AlexaFluor-488 utilized for all primary antibodies was determined by examining imaging wells and selecting settings that limited saturation. These imaging settings were utilized across all cell lines to allow for direct comparison and analysis. For imaging analysis, the sum fluorescence intensity was exported for each respective channel. Data was plotted using GraphPad Prism software.

Statistics

Statistical analysis was performed with the use of GraphPad Prism software (La Jolla, CA). Comparisons between two samples were performed with an unpaired t-test. One-way ANOVA was utilized for comparison between more than two samples. A two-sided p-value of < 0.05 was utilized to indicate significance. All experiments were performed a minimum of three times each.

Results

Expression in ovarian cancer

To first characterize the expression of ASIC2 in ovarian cancer, we queried ASIC2 mRNA expression across 617 ovarian tumors included in the TCGA database. Differentiating ASIC2 expression into quartiles and examining patient survival compared between low and high expression groups showed no significant change in survival. However, previous studies by our group have shown that overexpression of PDE10 in ovarian tumors did correlate with poor survival; therefore, we queried the expression of ASIC2 in the high PDE10 expression group compared to the PDE10 low group. As shown in Fig. 1A, as expected, PDE10 high expression confers a worse survival compared to PDE10 low consistent with previous work[11]. The significant difference ($p < 0.0001$) in expression between the PDE10 high and low groups is shown in Fig. 1B. Interestingly, ASIC2 expression was significantly higher in the PDE10 high group compared to the PDE10 low group ($p < 0.01$), Fig. 1C. We then measured baseline ASIC2 protein levels in human ovarian cancer cell lines by western blot as shown in Fig. 1D. Confocal IHC analysis confirmed that ASIC2 is expressed across ES2, SKOV3 and OVCAR8 cells, Fig. 1E–G. Furthermore, we observed ASIC2 expression appears to be localized primarily to the cellular nucleus in these ovarian cancer cells.

A potential role in ovarian cancer cell survival

In order to assess whether ASIC2 affected cancer cell viability, we performed growth assays by treating cells with known, non-specific ASIC ion channel inhibitors, Amiloride and Diminazene. Treatment of ES2, SKOV3 and OVCAR8 cells with Diminazene produced marked cell death with IC50 values as shown (Fig. 2A–C). However, SKOV3 cells were resistant to cell death despite treatment with Amiloride (Fig. 2B). Additionally, IC50 values in ES2 cells appear to be dramatically higher with Amiloride treatment than those with Diminazene (Fig. 2A), and slightly higher in OVCAR8 (Fig. 2C). Treatment of ES2, SKOV3, and OVCAR8 with ASIC2 inhibitors provoked a reduction in ASIC2 protein in all three cell lines as shown in Fig. 2D–F. Interestingly, this treatment also resulted in a reduction of PDE10 protein in ES2 cells, but not in SKOV3 or OVCAR8.

Previously generated PDE10-KO models[11], 5H5, 2 F4, and 2 C10 were analyzed for ASIC2 expression. Across all four clones tested, knockout of PDE10 resulted in a simultaneous decrease in ASIC2 protein expression (Fig. 3A). This relationship is most readily apparent in clone 2 C10, where a low-level expression of PDE10 shows a corresponding low expression of ASIC2 relative to other clones and the empty vector. Confocal IHC validated this trend (Fig. 3B). Specifically, nuclear levels of ASIC2 were investigated and noted to be significantly decreased across all PDE10-KO clones relative to the empty vector control (Fig. 3C). Additionally, all clones were tested for growth inhibition against Diminazene. As shown in Fig. 3D, PDE10-KO clones showed a decreased sensitivity to ASIC inhibition than the control cells.

ASIC2 mediates intracellular calcium and pH

As ASIC2 is a proton-mediated ion channel, we sought to analyze intracellular calcium upon treatment with Diminazene. Assessment of intracellular calcium levels was performed through the use of a fluorescent calcium probe across various time points. At 30 min, calcium levels were noted to be significantly increased in SKOV3 cells after ASIC2 inhibition, Fig. 4A,C. There was a small trend towards a similar increase in OVCAR8 cells, albeit this was not significant (Fig. 4A). As ASIC2 is proton gated and up-regulated in acidic conditions, we sought to determine if pH affected ASIC2 expression in ovarian cancer cell lines. Decreasing global extracellular pH to 6.0 and 6.5 across various time points from 2 to 24 h did not affect ASIC2 protein expression via western blot analysis (Supplemental Fig. 1). Therefore, we utilized a pH assay to determine intracellular changes in pH

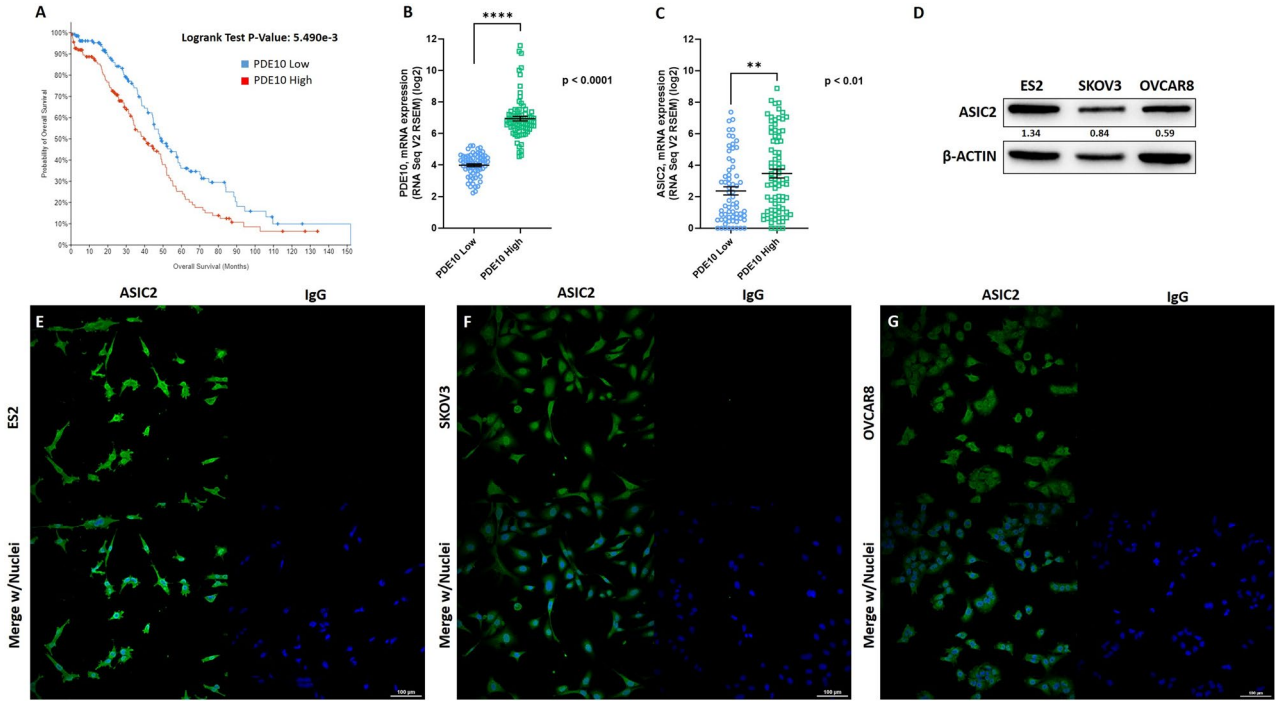

Fig. 1. ASIC2 correlation with PDE10. (**A**) Kaplan-Meier survival plot of PDE10 High and PDE10 Low mRNA expression in ovarian tumors from the TCGA. P-Value: 5.490e-3. (**B**) Expression of PDE10 mRNA in PDE10 High and PDE10 Low ovarian tumors. **** $P < 0.0001$. (**C**) ASIC2 expression in PDE10 High and PDE10 Low ovarian tumors. ** $P < 0.01$. (**D**) Western blot analysis of ASIC2 in ES2, SKOV3, and OVCAR8 cells. Quantification of ASIC2 is shown. β-ACTIN is used as a loading control. ASIC2 expression and localization in ovarian cancer cells. ASIC2 (Green, top left) or IgG control (top right) and merged with nuclei (Blue, bottom) for (**E**) ES2, (**F**) SKOV3, and (**G**) OVCAR8. Scale bar = 100 µm.

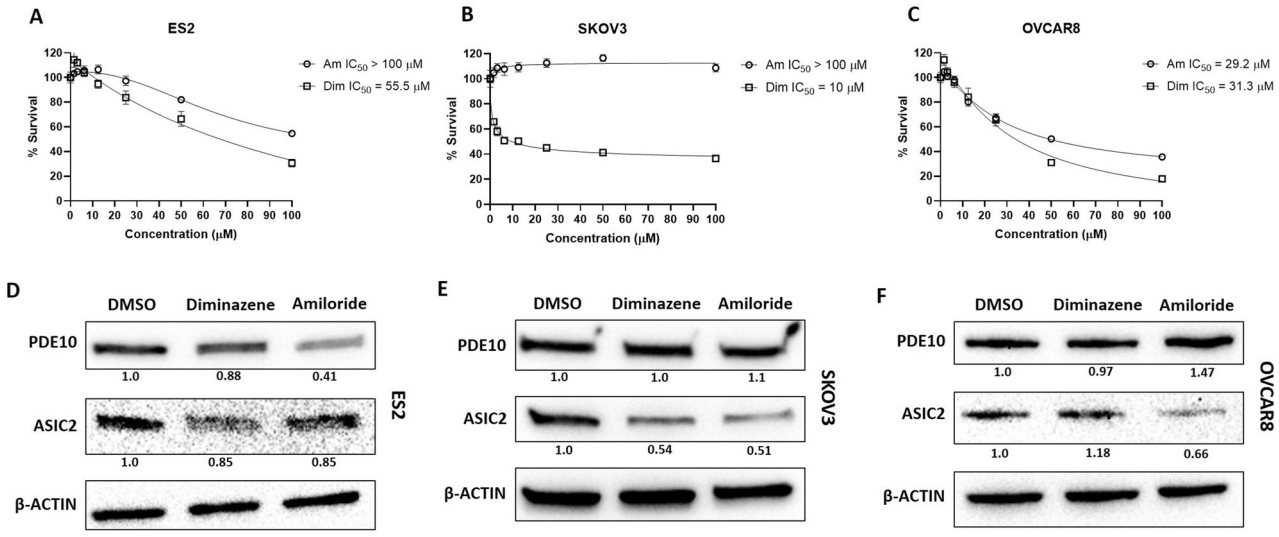

Fig. 2. Growth inhibition using ASIC2 inhibitors. Amiloride and Diminazene were analyzed for their ability to inhibit growth at multiple concentrations in (**A**) ES2, (**B**) SKOV3, and (**C**) OVCAR8. Cells were treated for 24 h with Diminazene (10 µM) and Amiloride (25 µM) and probed for expression of PDE10 and ASIC2. (**D**) PDE10 and ASIC2 are decreased with both diminazene and amiloride in ES2 cells. (**E**) PDE10 and ASIC2 are decreased with diminazene and amiloride in SKOV3 cells. (**F**) ASIC2 but not PDE10 is decreased with diminazene and amiloride in OVCAR8 cells. Quantification of PDE10 and ASIC2 blots is shown in **D**–**F**.

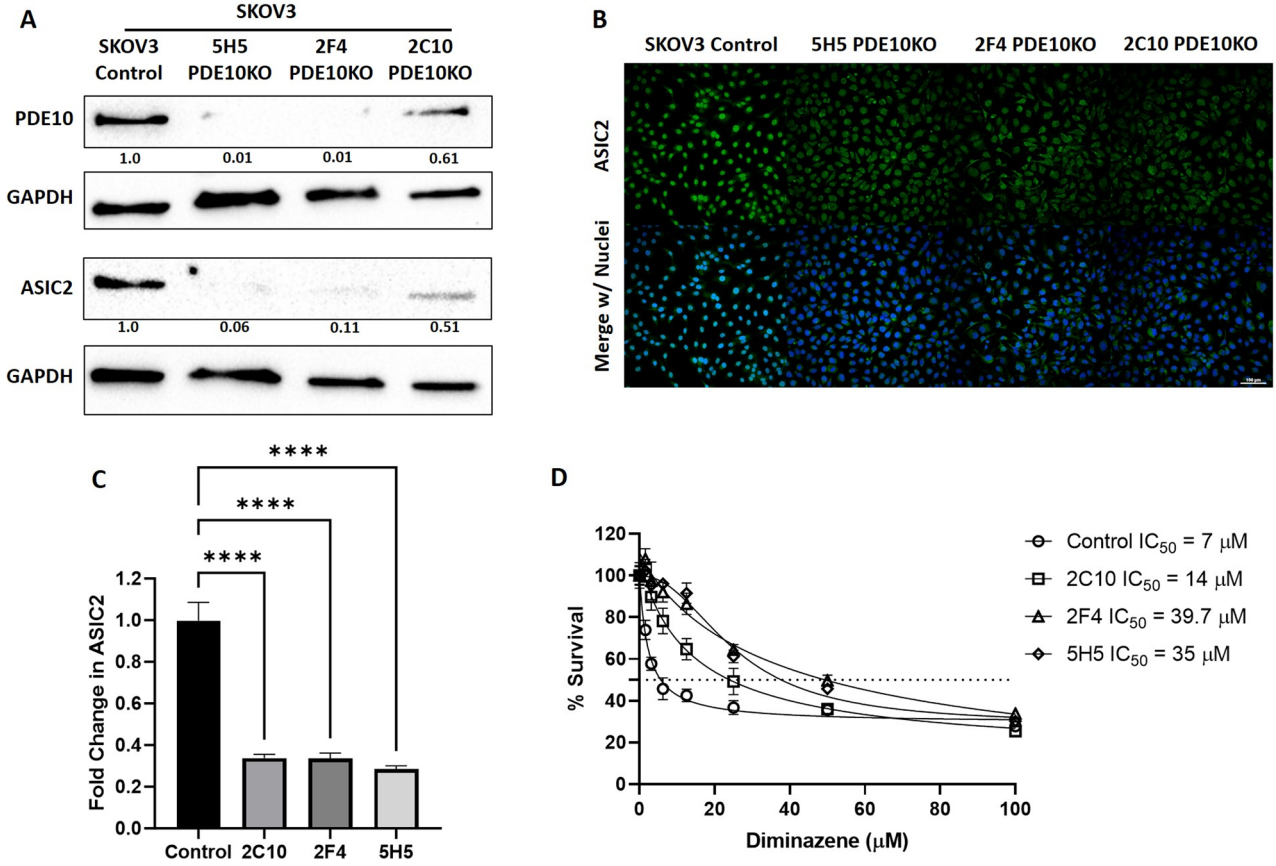

Fig. 3. ASIC2 expression in PDE10 knockout cells. (**A**) Previously generated SKOV3 PDE10 knockout cells were analyzed for expression of ASIC2 by western blot. GAPDH serves as a loading control. Quantification of PDE10 and ASIC2 is shown. (**B**) ASIC2 expression was analyzed by confocal immunofluorescence and is shown on top in green and on bottom merged with nuclei in blue. Scale bar = 100 μm. (**C**) Quantitative nuclear fluorescence analysis of cells in B show a statistically significant reduced expression of ASIC2 in PDE10 knockout cells. (**D**) PDE10-KO cells were analyzed for survival after treatment with Diminazene for 72 h. IC50 values for each clone is shown.

associated with ASIC2 expression. Intracellular pH was noted to increase with ASIC2 inhibition via Diminazene treatment, represented by a decrease in fluorescence (Fig. 4B). There was a statistically significant increase in pH at 30 min in SKOV3 cells (Fig. 4B,D) and a trend in OVCAR8 that did not fully reach significance; however, there was no difference in intracellular pH via ASIC inhibition in ES2 cells (Fig. 4B). Both pH as well as calcium concentration were back to levels of the controls after 2 h of treatment in all cells (Supplemental Fig. 2 A and 2B). For confirmation of increases in intracellular calcium, we analyzed changes in nuclear NFAT through confocal microscopy and quantification in Fig. 4E,H (SKOV3), Fig. 4F,I (ES2), and Fig. 4G,J (OVCAR8). We confirmed an increase in nuclear NFAT due to an increase in intracellular calcium through Diminazene treatment in SKOV3 cells (Fig. 4E,H) but not in ES2 (Fig. 4F,I) or OVCAR8 (Fig. 4G,J), respectively[23,24].

Downstream oncogenic signaling

The relationship between calcium and the Wnt/β-catenin signaling cascade has been well established previously[25]. Additionally, our previous work has shown phosphodiesterase blockade can prevent β-catenin nuclear localization and induces degradation and eventually cell death[11,26,27]. Due to the relationship of ASIC2 with PDE10, we next sought to determine if calcium signaling played a role in oncogenic β-catenin signaling in ovarian cancer cells. Treatment of SKOV3 cells with Diminazene showed a decrease in active S33/S37/T41 β-catenin (non-phospho S33/S37/T41) as shown by immunofluorescence (Fig. 5A). After quantification, this was a significant decrease (Fig. 5D). However, no change was seen in OVCAR8 (Fig. 5B,E) or in ES2 cells (Fig. 5C–F). Interestingly, no significant change was noted in active S45 β-catenin (non-phospho S45) in any cell lines tested as shown in Supplemental Fig. 3.

Next, we analyzed PDE10-KO clones for expression of β-catenin at all phosphorylation sites. As seen in Fig. 6A, a decrease was seen in active S45 β-catenin that reached significance in all clones after quantification in Fig. 6C. Additionally, a decrease in active S33/S37/T41 β-catenin was seen in all clones (Fig. 6B), however significance was only seen in 2 C10 and 2 F4 after quantification (Fig. 6D).

β-catenin is known to act as a transcription factor along with TCF/LEF to induce the expression of the oncogene MYC[28]. PDE10-KO clones were analyzed for expression of C-MYC by immunofluorescence. As

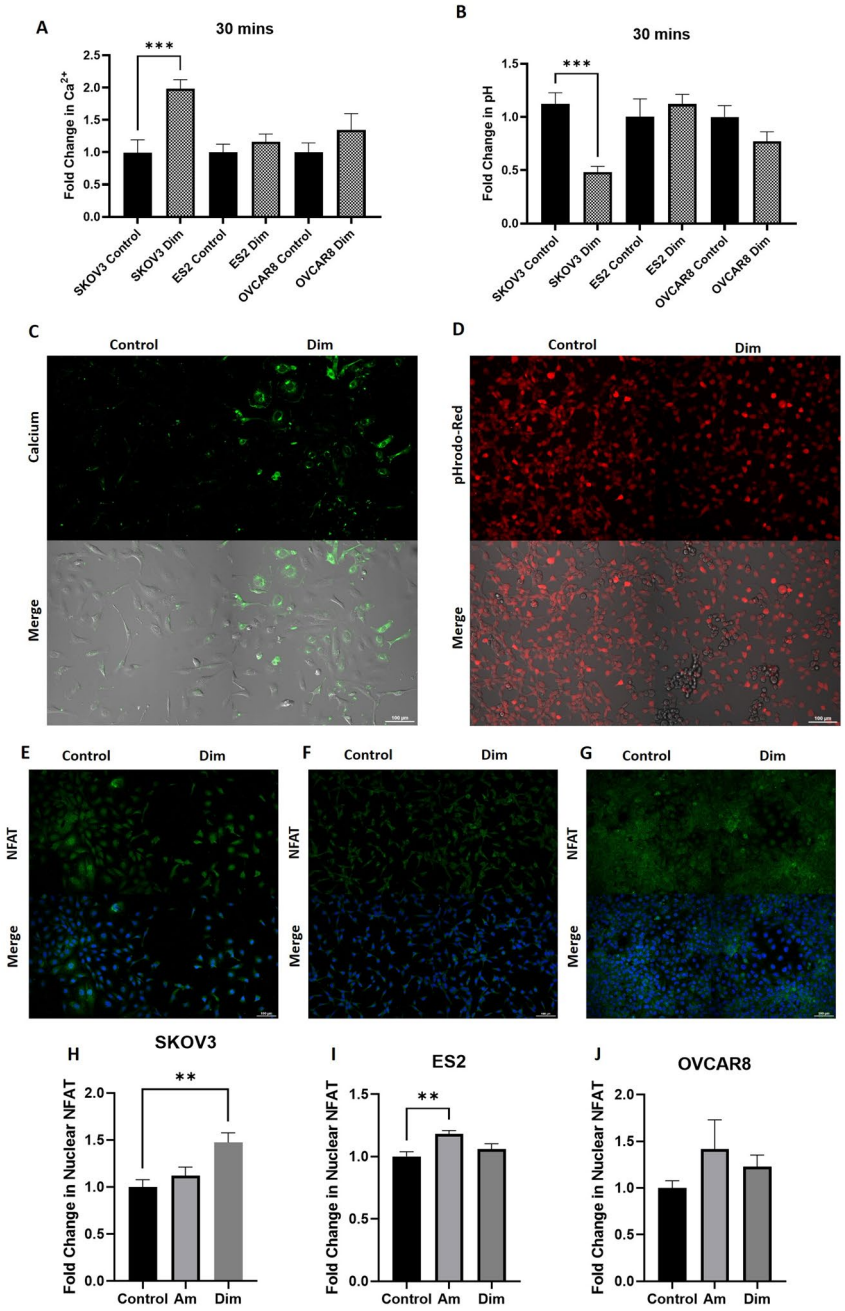

Fig. 4. Intracellular calcium and pH analysis. Fluo-5 F calcium indicator was used to analyze intracellular calcium levels. SKOV3 showed a significant increase in calcium when treated with Diminazene (10 μM) at 30 min (**A**). pHrodo red pH indicator is inversely proportional to pH such that an increase in pH is represented by a decrease in fluorescence. SKOV3 showed a significant increase in pH when treated with Diminazene (10 μM) at 30 min (**B**). **C** Representative images of SKOV3 cells treated with Diminazene vs. control showing an increase in fluorescence corresponding to calcium increase. **D** Representative images of SKOV3 treated with Diminazene vs. control showing a decrease in fluorescence of pHrodo-Red indicating an increase in pH. Fluorescence images of NFAT are shown for **E** SKOV3, **F** ES2, and **G** OVCAR8. Nuclear quantification of NFAT fluorescence is shown for **H** SKOV3 cells, **I** ES2, and **J** OVCAR8. Scale bar = 100 μm.

seen in Fig. 7A, PDE10-KO clones showed a decreased expression of C-MYC. Nuclear quantification showed a significant down regulation of C-MYC in two of the clones, Fig. 7B. We next analyzed the ASIC2 promoter for C-MYC binding sites as a transcription factor. As shown in Fig. 7C, the previously described ASIC2 promoter[29] contains two sites for MYC binding in the highlighted region. These two areas are consistent with previously published consensus sequences for C-MYC binding as a transcription factor (Fig. 7D)[30]. This work suggests that the interaction between ASIC2 and PDE10 in EOC may converge at β-catenin signaling.

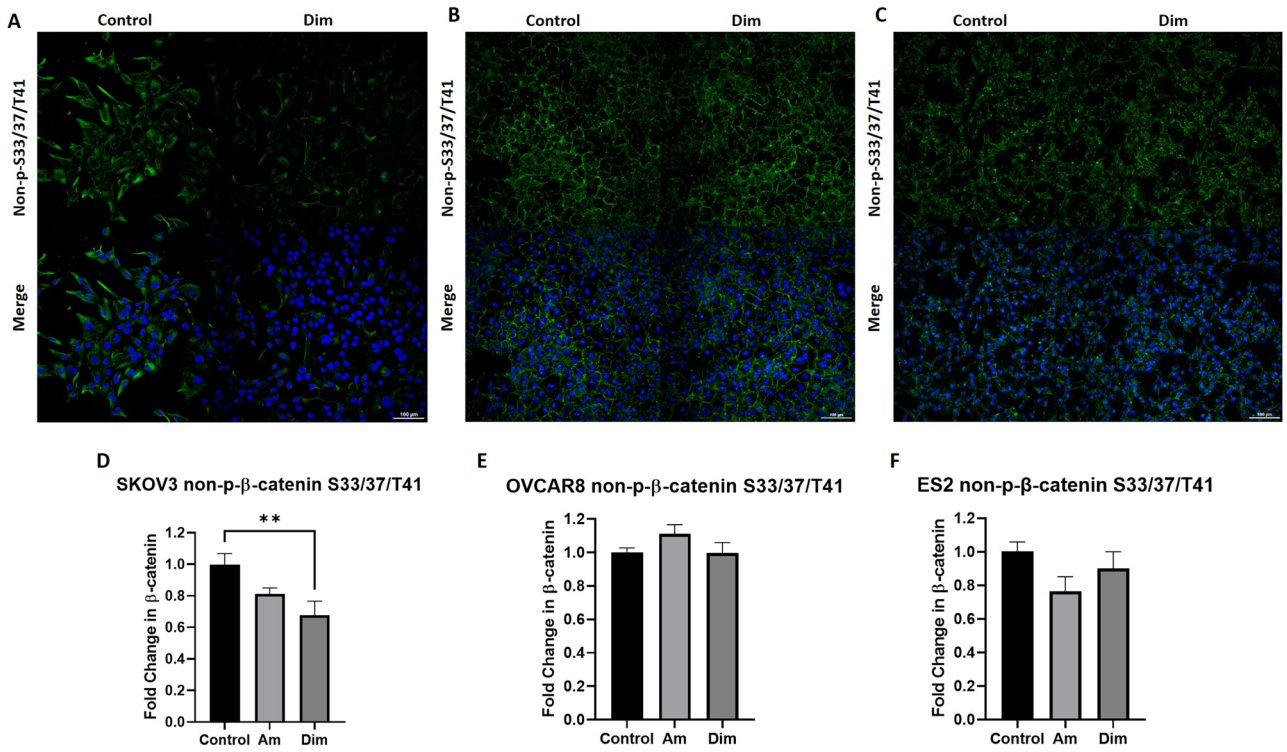

Fig. 5. β-catenin signaling with ASIC inhibition. Cells treated with Diminazene were probed for non-phospho β-catenin at S33/37/T41 for (**A**) SKOV3, (**B**) OVCAR8, and (**C**) ES2. Quantification of fluorescence is shown for (**D**) SKOV3, (**E**) OVCAR8, and (**F**) ES2. Scale bar = 100 µm.

Discussion

A poor understanding of the pathogenesis of ovarian cancer has limited our efforts at early detection and prevention. Recent data have shown that the inflammatory environment shared by the ovary and distal FT during ovulatory events is integral to the development of ovarian cancer[31,32]. Exposure of the FT to follicular fluid can induce cytokines, reactive oxygen species (ROS) and other growth factors leading to an increased risk for ovarian cancer[32].

NSAIDs are suggested to have a benefit in decreasing the risk of EOC, further underscoring the importance of inflammation and the immune response[32,33]. The anticancer properties of NSAIDs may be COX-independent and act through the inhibition of PDEs, specifically PDE10 in the ovary. We recently showed that PDE10 inhibition via ADT 061 treatment may interrupt or modify EOC tumorigenesis[11]. Here, we show that PDE10 may also affect ASIC2, an ion channel that may be integral in the context of inflammation and extracellular acidification.

To date, most ASIC ion channel study has been in the context of the central nervous system. Ischemic injury, trauma and cancer are known to cause tissue acidosis and inflammation and thereby, activate ASIC receptors[34]. Activated channels then allow for the influx of cations with changes in pH levels[16]. For instance, ASIC1a can be activated during brain ischemia and increase neuronal injury by leading to calcium overload[35].

While ASICs are well-studied with critical roles in acidosis and inflammation, little is known about ASIC channels in the acidic tumor microenvironment, particularly in ovarian cancer. Here, we report that ASIC2 is expressed in ovarian cancer, both in vitro and in vivo as assessed through the TCGA database. Our results further validate the findings of Zhou et al. who found that ASIC2 can promote growth and metastasis of CRC under acidic conditions[21]. The ASIC inhibitors used in our studies will inhibit ASIC1, ASIC2, and ASIC3. However, ASIC1 and ASIC2 both showed differential expression in the TCGA database when comparing PDE10 Low vs. PDE10 High, yet upon western blot analysis of ASIC1 we found no expression (Supplemental Fig. 9). ASIC3 showed no significant differential expression in the TCGA analysis (Supplemental Fig. 9). For these reasons we focused on ASIC2 for our studies.

Interestingly, our results also show that the expression of ASIC2 is positively correlated with PDE10 in ovarian tumors. We further validated this interplay between ASIC2 and PDE10 by analyzing ASIC2 in a PDE10 genetic knock-down model. It appears that decreasing PDE10 also results in a decreased expression of ASIC2 in EOC cells. To the best of our knowledge, this relationship has not been previously reported in literature, particularly in the context of ovarian cancer.

While changing the global extracellular pH did not affect ASIC2 expression, intracellular pH and calcium levels were significantly altered by inhibiting the function of this ion channel. Notably, cytosolic calcium was increased likely due to the presence of ASIC2 on or around the nucleus as depicted in Fig. 7 whereby inhibition of ASIC2 shuts down the tightly regulated calcium flow within the cell[36]. This was most notably observed in SKOV3

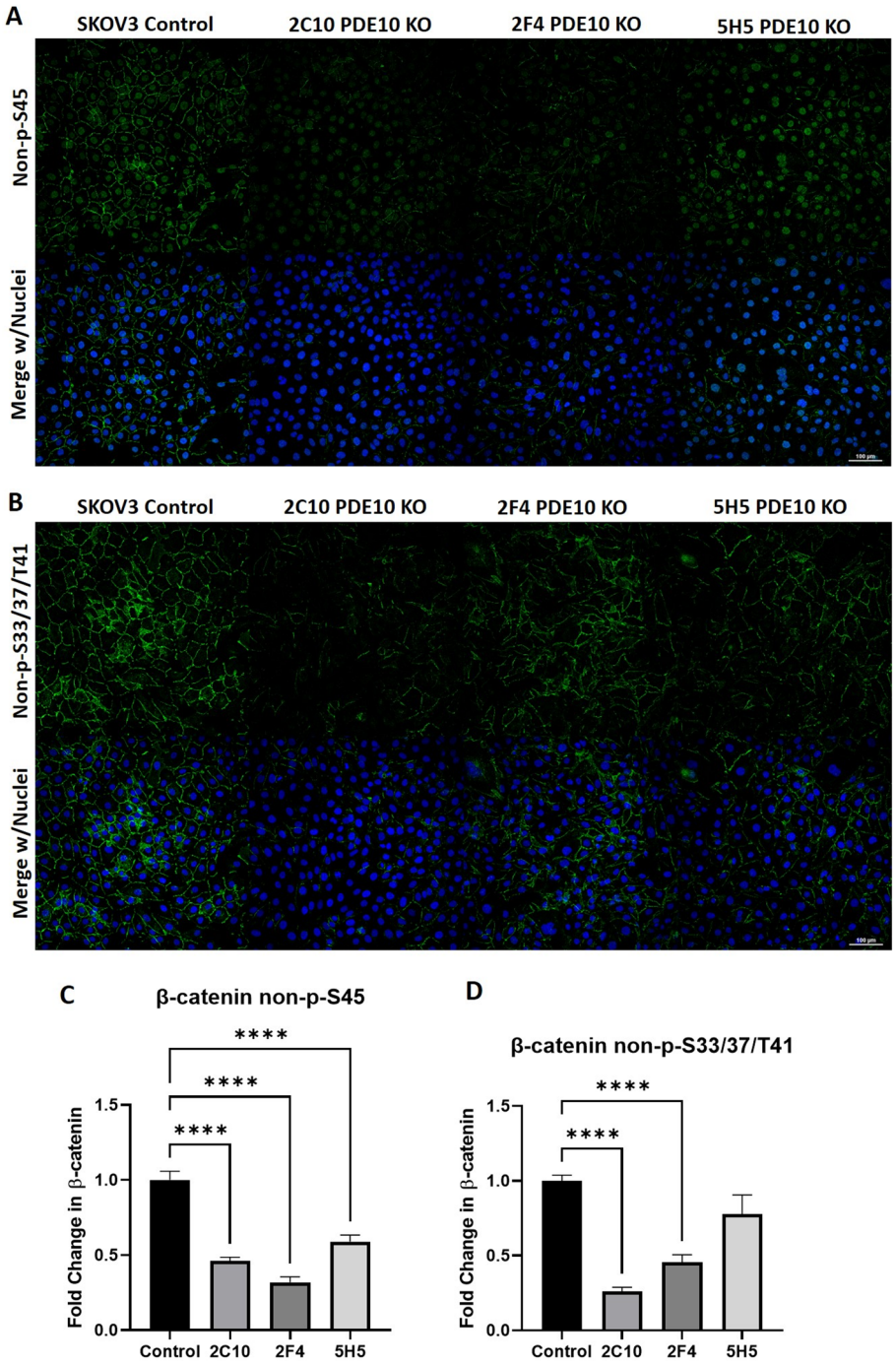

Fig. 6. β-catenin signaling in PDE10-KO cells. (**A**) SKOV3 PDE10-KO cells probed for non-phospho β-catenin at S45. (**B**) SKOV3 PDE10-KO cells probed for non-phospho β-catenin at S33/37/T41. (**C**) Quantification of fluorescence in (**A**) **D** Quantification of fluorescence in (**B**) Scale bar = 100 µm.

and a similar trend was noted in OVCAR8 cells, albeit not statistically significant. This may be potentially due to the differences in basal ASIC2 expression and IC50 values needed to produce an effect between cell lines. Notably, SKOV3 cells were much more sensitive to Diminazene treatment at 10 µM than either OVCAR8 or ES2 cells which required much higher concentrations to achieve the same cell growth inhibition. A consistent effect was seen for each cell line in response to the interventions used. Additionally, we found the influx of calcium to affect oncogenic β-catenin signaling at S33/37/T41, but not at S45. Other reports show calcium induces PKC activation which phosphorylates β-catenin at these sites leading to degradation[37]. However, the knockout of PDE10 not only showed a decrease in β-catenin at S33/37/T41, but S45 as well. This suggests the convergence of the two pathways, ASIC2 and PDE10, on β-catenin. Because of this and the promoter analysis in Fig. 7 we propose that MYC regulates the expression of ASIC2 in ovarian cancer, and can be modified through its activity

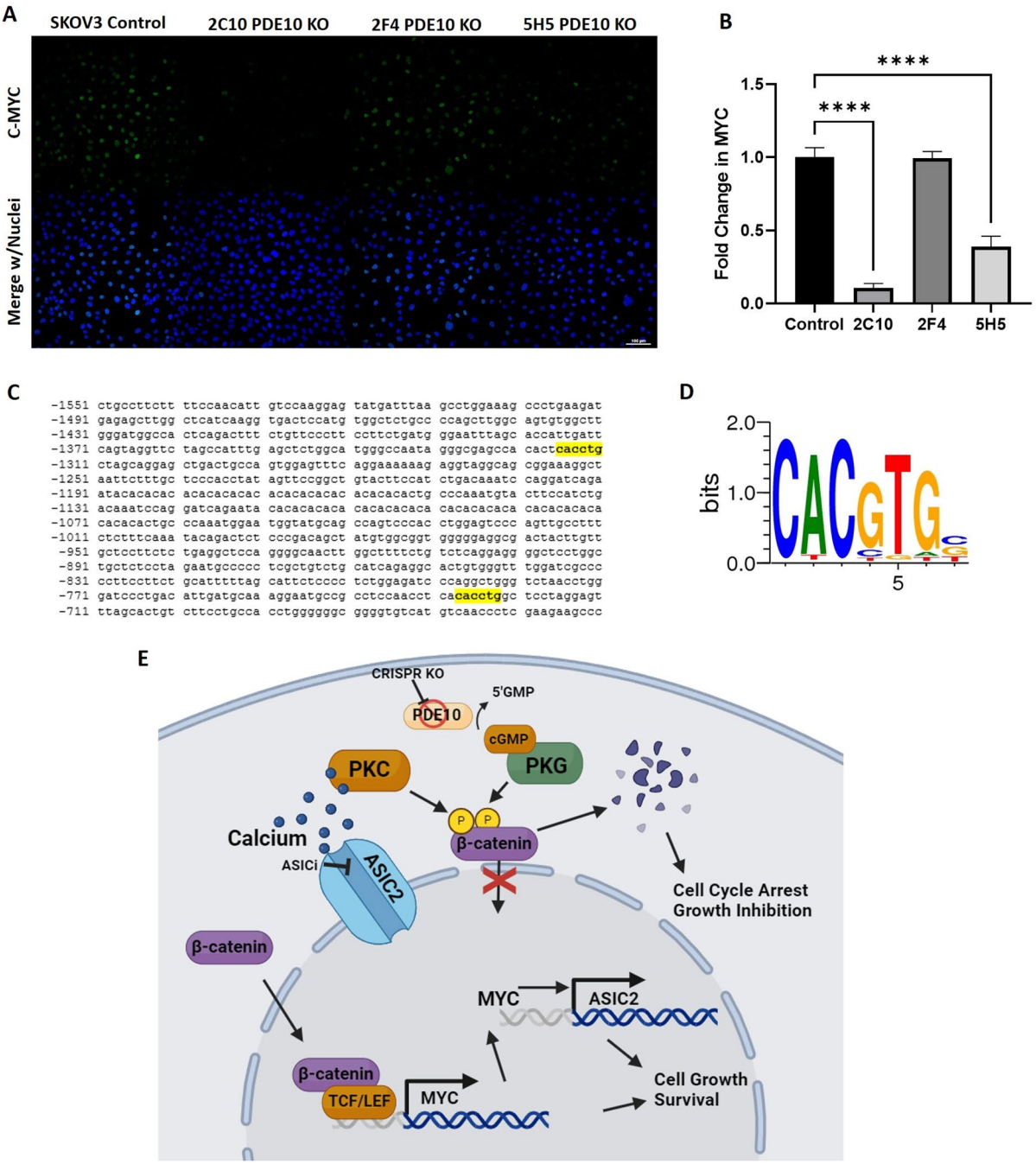

Fig. 7. Downstream ASIC signaling in ovarian cancer. (**A**) SKOV3 PDE10-KO cells were probed for expression of C-MYC. (**B**) Quantification of nuclear C-MYC expression from A. (**C**) Promoter region of ASIC2 containing highlighted MYC binding sites. (**D**) Previously published consensus binding site of MYC[29]. (**E**) Proposed signaling pathway describing the relationship between ASIC2 and PDE10 through the convergence on β-catenin and mediated by MYC. Scale bar = 100 μm.

(Fig. 7E). The results reported here demonstrate that there is a direct relationship between ASIC2 and PDE10, which appears to be critical for cancer cell viability. We hypothesize that ASIC2 may therefore play an integral role in acidosis-mediated cancer cell survival and progression through signaling from a potential acidic tumor microenvironment into the nucleus of cancer cells through a β-catenin mediated pathway.

Data availability

The data generated in this study are available within this article and its supplementary data files.

Received: 28 January 2025; Accepted: 20 May 2025

Published online: 28 May 2025

References

1. Colombo, N. et al. Ovarian cancer. *Crit. Rev. Oncol. Hematol.* **60**, 159–179. https://doi.org/10.1016/j.critrevonc.2006.03.004 (2006).
2. Coleman, R. L., Monk, B. J., Sood, A. K. & Herzog, T. J. Latest research and treatment of advanced-stage epithelial ovarian cancer. *Nat. Rev. Clin. Oncol.* **10**, 211–224. https://doi.org/10.1038/nrclinonc.2013.5 (2013).
3. Kroeger, P. T. & Drapkin, R. Pathogenesis and heterogeneity of ovarian cancer. *Curr. Opin. Obstet. Gynecol.* **29**, 26–34. https://doi.org/10.1097/GCO.0000000000000340 (2017).
4. Nyoman Gede Budiana, I. Ovarian cancer: Pathogenesis and current recommendations for prophylactic surgery. *J. Turk.-German Gynecol. Assoc.* https://doi.org/10.4274/jtgga.galenos.2018.2018.0119 (2018).
5. Nik, N. N., Vang, R., Shih, I-M. & Kurman, R. J. Origin and pathogenesis of pelvic (Ovarian, tubal, and primary Peritoneal) serous carcinoma. *Annu. Rev. Pathol.* **9**, 27–45. https://doi.org/10.1146/annurev-pathol-020712-163949 (2014).
6. Kang, M. et al. Ovarian BDNF promotes survival, migration, and attachment of tumor precursors originated from p53 mutant fallopian tube epithelial cells. *Oncogenesis* **9**, 1–15. https://doi.org/10.1038/s41389-020-0243-y (2020).
7. Zhang, D., Bai, B., Xi, Y., Wang, T. & Zhao, Y. *Is aspirin use associated with a decreased risk of ovarian cancer? A systematic review and meta-analysis of observational studies with dose-response analysis* (Academic Press Inc., 2016).
8. Murphy, M. A. et al. Non-steroidal anti-inflammatory drug use and ovarian cancer risk: findings from the NIH-AARP diet and health study and systematic review. *Cancer Causes Control.* **23**, 1839–1852. https://doi.org/10.1007/s10552-012-0063-2 (2012).
9. Trabert, B. et al. Aspirin, nonaspirin nonsteroidal anti-inflammatory drug, and acetaminophen use and risk of invasive epithelial ovarian cancer: A pooled analysis in the ovarian cancer association consortium. *J. Natl Cancer Inst.* https://doi.org/10.1093/jnci/djt431 (2014).
10. Thompson, W. J. et al. Exisulind induction of apoptosis involves Guanosine 3′,5′-Cyclic monophosphate phosphodiesterase Inhibition, protein kinase G activation, and attenuated β-Catenin. *Cancer Res.* **60**, 3338–3342 (2000).
11. Borneman, R. M. et al. Phosphodiesterase 10A (PDE10A) as a novel target to suppress β-catenin and RAS signaling in epithelial ovarian cancer. *J. Ovarian Res.* **15**, 120. https://doi.org/10.1186/s13048-022-01050-9 (2022).
12. Wang, Y-Z. et al. Intracellular ASIC1a regulates mitochondrial permeability transition-dependent neuronal death. *Cell. Death Differ.* **20**, 1359–1369. https://doi.org/10.1038/cdd.2013.90 (2013).
13. Ruan, N. et al. Acid-Sensing ion channels and mechanosensation. *Int. J. Mol. Sci.* **22**, 4810. https://doi.org/10.3390/ijms22094810 (2021).
14. Price, M. P. et al. Localization and behaviors in null mice suggest that ASIC1 and ASIC2 modulate responses to aversive stimuli. *Genes Brain Behav.* **13**, 179–194. https://doi.org/10.1111/gbb.12108 (2014).
15. Storozhuk, M., Cherninskyi, A., Maximyuk, O., Isaev, D. & Krishtal, O. Acid-sensing ion channels: Focus on physiological and some pathological roles in the brain. *Curr. Neuropharmacol.* **19**, 1570–1589. https://doi.org/10.2174/1570159X19666210125151824 (2017).
16. Kweon, H-J. & Suh, B-C. Acid-sensing ion channels (ASICs): therapeutic targets for neurological diseases and their regulation. *BMB Rep.* **46**, 295–304. https://doi.org/10.5483/BMBRep.2013.46.6.121 (2013).
17. Pignataro, G., Simon, R. P. & Xiong, Z-G. Prolonged activation of ASIC1a and the time window for neuroprotection in cerebral ischaemia. *Brain* **130**, 151–158. https://doi.org/10.1093/brain/awl325 (2007).
18. Zhang, L. et al. Pathology and physiology of acid–sensitive ion channels in the digestive system (Review). *Int. J. Mol. Med.* **50**, 1–12. https://doi.org/10.3892/ijmm.2022.5150 (2022).
19. Zhu, S. et al. ASIC1 and ASIC3 contribute to acidity-induced EMT of pancreatic cancer through activating Ca2+/RhoA pathway. *Cell. Death Dis.* **8**, e2806–e2806. https://doi.org/10.1038/cddis.2017.189 (2017).
20. Gupta, S. C. et al. Regulation of breast tumorigenesis through acid sensors. *Oncogene* **35**, 4102–4111. https://doi.org/10.1038/onc.2015.477 (2016).
21. Zhou, Z. et al. The acid-sensing ion channel, ASIC2, promotes invasion and metastasis of colorectal cancer under acidosis by activating the calcineurin/NFAT1 axis. *J. Experimental Clin. Cancer Res.* **36**, 130. https://doi.org/10.1186/s13046-017-0599-9 (2017).
22. Kapoor, N. et al. Interaction of ASIC1 and ENaC subunits in human glioma cells and rat astrocytes. *Am. J. Physiology-Cell Physiol.* **300**, C1246–C1259. https://doi.org/10.1152/ajpcell.00199.2010 (2011).
23. Sharma, S. et al. Dephosphorylation of the nuclear factor of activated T cells (NFAT) transcription factor is regulated by an RNA-protein scaffold complex. *Proc. Natl. Acad. Sci.* **108**, 11381–11386. https://doi.org/10.1073/pnas.1019711108 (2011).
24. Tomida, T., Hirose, K., Takizawa, A., Shibasaki, F. & Iino, M. NFAT functions as a working memory of Ca2 + signals in decoding Ca2 + oscillation. *EMBO J.* **22**, 3825–3832. https://doi.org/10.1093/emboj/cdg381 (2003).
25. Komiya, Y. & Habas, R. Wnt signal transduction pathways. *Organogenesis* **4**, 68–75 (2008).
26. Lee, K. et al. β-catenin nuclear translocation in colorectal cancer cells is suppressed by PDE10A Inhibition, cGMP elevation, and activation of PKG. *Oncotarget* **7**, 5353–5365. https://doi.org/10.18632/oncotarget.6705 (2016).
27. Lee, K. J. et al. Suppression of Colon tumorigenesis in mutant apc mice by a novel PDE10 inhibitor that reduces oncogenic β-Catenin. *Cancer Prev. Res. (Phila).* **14**, 995–1008. https://doi.org/10.1158/1940-6207.CAPR-21-0208 (2021).
28. Rennoll, S. & Yochum, G. Regulation of MYC gene expression by aberrant Wnt/β-catenin signaling in colorectal cancer. *World J. Biol. Chem.* **6**, 290–300. https://doi.org/10.4331/wjbc.v6.i4.290 (2015).
29. Xia, J. et al. Molecular cloning and characterization of human acid sensing ion channel (ASIC)2 gene promoter. *Gene* **313**, 91–101. https://doi.org/10.1016/S0378-1119(03)00633-4 (2003).
30. Allevato, M. et al. Sequence-specific DNA binding by MYC/MAX to low-affinity non-E-box motifs. *PLOS ONE.* **12**, e0180147. https://doi.org/10.1371/journal.pone.0180147 (2017).
31. Jia, D., Nagaoka, Y., Katsumata, M. & Orsulic, S. Inflammation is a key contributor to ovarian cancer cell seeding. *Sci. Rep.* **8**, 12394. https://doi.org/10.1038/s41598-018-30261-8 (2018).
32. Savant, S. S., Sriramkumar, S. & O'Hagan, H. M. The role of inflammation and inflammatory mediators in the development, progression, metastasis, and chemoresistance of epithelial ovarian Cancer. *Cancers* **10**, 251. https://doi.org/10.3390/cancers10080251 (2018).
33. Prizment, A. E., Folsom, A. R. & Anderson, K. E. Nonsteroidal Anti-Inflammatory drugs and risk for ovarian and endometrial cancers in the Iowa women's health study. *Cancer Epidemiol. Biomarkers Prev.* **19**, 435–442. https://doi.org/10.1158/1055-9965.EPI-09-0976 (2010).
34. Foster, V. S., Rash, L. D., King, G. F. & Rank, M. M. Acid-sensing ion channels: Expression and function in resident and infiltrating immune cells in the central nervous system. *Front. Cell. Neurosci.* https://doi.org/10.3389/fncel.2021.738043 (2021).
35. Xiong, Z-G. & Xu, T-L. The role of asics in cerebral ischemia. *Wiley Interdisciplinary Reviews: Membrane Transp. Signal.* **1**, 655–662. https://doi.org/10.1002/wmts.57 (2012).
36. Clapham, D. E. & Calcium Signaling *Cell* ;**131**: 1047–1058. doi:https://doi.org/10.1016/j.cell.2007.11.028 (2007).
37. Gwak, J. et al. Protein-kinase-C-mediated β-catenin phosphorylation negatively regulates the Wnt/β-catenin pathway. *J. Cell Sci.* **119**, 4702–4709. https://doi.org/10.1242/jcs.03256 (2006).

Author contributions

TJ, SC, AW, MHS, EC, and KL were involved in generating data for the manuscript. TJ, SC, and KL wrote the initial text and prepared all figures. JS provided editorial and mentor expertise while overseeing direction of studies. All authors edited and reviewed the manuscript prior to submission.

Funding

These studies were funded by the USA Health Mitchell Cancer Institute. No external funding was used for these studies.

Declarations

Competing interests

All authors declare no potential conflicts of interest. The authors declare no competing interests.

Additional information

Supplementary Information The online version contains supplementary material available at https://doi.org/10.1038/s41598-025-03429-2.

Correspondence and requests for materials should be addressed to K.J.L.

Reprints and permissions information is available at www.nature.com/reprints.

Publisher's note Springer Nature remains neutral with regard to jurisdictional claims in published maps and institutional affiliations.